



Controlled Phase Shifts with a Single Quantum Dot

Ilya Fushman, *et al.*
Science **320**, 769 (2008);
DOI: 10.1126/science.1154643

The following resources related to this article are available online at www.sciencemag.org (this information is current as of June 29, 2009):

Updated information and services, including high-resolution figures, can be found in the online version of this article at:

<http://www.sciencemag.org/cgi/content/full/320/5877/769>

Supporting Online Material can be found at:

<http://www.sciencemag.org/cgi/content/full/320/5877/769/DC1>

This article **cites 23 articles**, 2 of which can be accessed for free:

<http://www.sciencemag.org/cgi/content/full/320/5877/769#otherarticles>

This article has been **cited by** 4 article(s) on the ISI Web of Science.

This article appears in the following **subject collections**:

Physics, Applied

http://www.sciencemag.org/cgi/collection/app_physics

Information about obtaining **reprints** of this article or about obtaining **permission to reproduce this article** in whole or in part can be found at:

<http://www.sciencemag.org/about/permissions.dtl>

Controlled Phase Shifts with a Single Quantum Dot

Ilya Fushman,^{1*} Dirk Englund,^{1*} Andrei Faraon,^{1*} Nick Stoltz,² Pierre Petroff,² Jelena Vučković^{3†}

Optical nonlinearities enable photon-photon interaction and lie at the heart of several proposals for quantum information processing, quantum nondemolition measurements of photons, and optical signal processing. To date, the largest nonlinearities have been realized with single atoms and atomic ensembles. We show that a single quantum dot coupled to a photonic crystal nanocavity can facilitate controlled phase and amplitude modulation between two modes of light at the single-photon level. At larger control powers, we observed phase shifts up to $\pi/4$ and amplitude modulation up to 50%. This was accomplished by varying the photon number in the control beam at a wavelength that was the same as that of the signal, or at a wavelength that was detuned by several quantum dot linewidths from the signal. Our results present a step toward quantum logic devices and quantum nondemolition measurements on a chip.

Photons are attractive candidates for quantum bits, because they do not interact strongly with their environment and can be transmitted over long distances. They are well suited for carrying information by means of polarization or photon number, and can be manipulated with great precision by optical elements (1). In addition, photonic qubits can be used to interconnect atom-like qubits realized in various systems (2–6). Quantum logic with photons requires a gate that facilitates an interaction between two coincident photons (7). A controlled-phase gate, which can be realized by an atom in a high-quality (Q) cavity (2), performs this function. In this gate, the accumulated phase of one beam is dependent on the total number of photons interacting with the atom, and the presence of other photons can be measured without destroying them (8–10).

Our nonlinear medium consisted of a three-hole-defect photonic crystal (PC) cavity (11) with a coupled InAs quantum dot (QD) (Fig. 1A). Because of the presence of a distributed Bragg reflector underneath the PC membrane, we treated the PC cavity as a one-sided system. The structure was thermally isolated, allowing us to control the cavity and QD resonances with a heating laser (12). The cavity field decay rate was $\kappa/2\pi = 16\text{GHz}$, corresponding to a quality factor $Q = 10,000$. The QD had an estimated spontaneous emission rate of $\gamma/2\pi = 0.2\text{GHz}$. In the described experiments, we employed two QDs: a strongly coupled QD with a vacuum Rabi frequency $g/2\pi = 16\text{GHz}$ and a weakly coupled QD with $g/2\pi = 8\text{GHz}$.

We measured the phase of cavity-reflected beams by interfering them with a reference beam of known amplitude and phase (Fig. 1A).

The reflectivity of the linearly polarized cavity was isolated from background laser scatter by means of a cross-polarized setup (13, 12). The reference beam was introduced by inserting a quarter wave plate (QWP) between the beam-splitter and the cavity. The QWP converted the linearly polarized signal into an elliptically polarized beam with components parallel and orthogonal to the cavity polarization. After reflection from the sample, these two components acquired a relative phase. The detected signal I_s is an interference between the cavity-reflected component and the reference field

$$I_s(\omega) = \left| A(\theta) \left[r(\omega) + e^{i\Psi(\theta)} \right] \right|^2 \quad (1)$$

where $A(\theta)$ is a coefficient that depends on the QWP angle θ relative to the vertical polarization of the polarizing beam splitter (PBS), $r(\omega)$ is the frequency and power-dependent cavity reflectivity, and $\Psi(\theta)$ is the reference phase delay. $A(\theta)$, $r(\omega)$, and $\Psi(\theta)$ are given in the supporting online material (SOM).

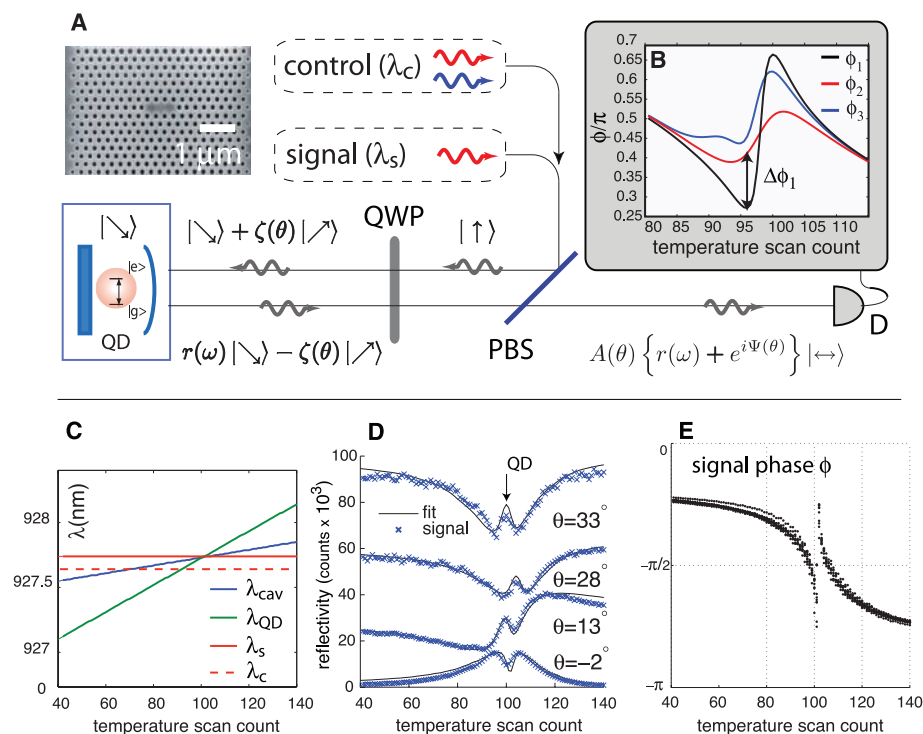


Fig. 1. Experimental setup (A). Vertically polarized control (wavelength λ_c) and signal (wavelength λ_s) beams are sent to the PC cavity (inset) via a PBS. A QWP (fast axis θ from vertical) changes the relative phase and amplitude $[\zeta(\theta)]$ of components polarized along and orthogonal to the cavity. Only the reflection coefficient $r(\omega)$ for cavity-coupled light (at $\sim 45^\circ$) depends on the input frequency and amplitude. The PBS transmits horizontally polarized light to a detector, D. (B) Theoretical model for the phase of signal beam ϕ . The signal phase ϕ_1 changes to ϕ_2 or ϕ_3 when the control and signal beams are resonant or detuned, respectively, and $n_c = 0.3$. The nonlinear phase shift due to the increase in power is shown as $\Delta\phi_1$. The wavelength detuned control shifts the phase ϕ_3 relative to ϕ_1 by the ac Stark effect (19). ϕ_3 is asymmetric because the cavity-coupled control power depends on the cavity and QD wavelengths during the temperature scan (C) (see SOM). The temperature was scanned from 20 to 27 K. (D) Measured R for different QWP angles and fit by theoretical model Eq. 1. (E) Phase of the reflected beam, extracted from the model fits in (D).

¹Applied Physics, Stanford University, Stanford, CA 94305, USA. ²Electrical and Computer Engineering, University of California, Santa Barbara, CA 93106, USA. ³Electrical Engineering, Stanford University, Stanford, CA 94305, USA.

*These authors contributed equally to this work.

†To whom correspondence should be addressed. E-mail: jela@stanford.edu

We first performed phase measurements on a single (signal) beam reflected from the cavity with a QD. Interference between the QD-scattered field and the incident signal resulted in the rapidly varying feature in Fig. 1D. As the phase of the reference beam increased from 0° to 33° , this interference evolved from destructive to constructive, and the dip at $\theta = 0^\circ$ changed to a peak at $\theta = 33^\circ$. We find that this interference is only explained by coherent light scattering from the QD. The experimental data are fit well by Eq. 1, as shown in Fig. 1D. Each fit gives the signal phase $\phi = \arctan(\Im[r(\omega)]/\Re[r(\omega)])$, where $\Re[r(\omega)]$ and $\Im[r(\omega)]$ are the real and imaginary parts of the cavity reflectivity $r(\omega)$. The phase fits for 11 scans with different QWP angles θ are superposed in Fig. 1E. As the signal wavelength traverses the cavity resonance, ϕ changes from 0 to $-\pi$. An additional phase modulation occurs at the QD resonance, where the phase varies by almost π over the dot bandwidth ($2g^2/\kappa = 2\pi \times 32$ GHz).

When measuring the controlled-phase shifts, we first considered the cases in which the control and signal have the same wavelength (they potentially could be distinguished by polarization or incident direction). When the control and signal are at the same wavelength, the nonlinear interaction between them (Fig. 2, A and B) arises from the saturation of the QD in the presence of cavity-coupled photons (12). Saturation occurs when the average photon number inside the cavity reaches approximately one photon per modified QD lifetime, given by κ/g^2 . The cavity photon number is $n_c = \eta P_{\text{in}}/[2\kappa\hbar\omega_c]$, given the input power P_{in} , control frequency ω_c , and coupling efficiency $\eta \approx 2$ to 5% in our experimental setup. The observed QD-induced dip does not fully reach zero at low powers, as expected from theory (12, 14), because of QD-wavelength jitter and blinking (see SOM).

We observed a phase modulation of 0.24π (43°) when the control photon number was increased from $n_c = 0.08$ to 3 and the wavelength was set 0.014 nm ($g/3.5$) away from the anti-crossing point (Fig. 2C). The reflectivity amplitude R normalized by the cavity reflectivity without a dot R_0 is shown for the same detuning in Fig. 2E and changed from 50 to 100% at saturation. The excitation powers were 40 nW and 1.3 μ W, measured before the objective lens (corresponding to n_c of 0.08 and 3, respectively), and indicate a coupling efficiency of up to 5%. However, the coupling efficiency fluctuated because of sample drift during the experiment. Therefore, we estimate control powers from fits to the data, and give power levels measured before the objective lens for reference.

In the context of quantum gates (2, 15, 16), we are interested in the signal photon's phase change caused by a single control photon. When the control and signal have the same wavelength ($\lambda_c = \lambda_s$) and the same duration, the change is given by the difference between the phase evaluated at n_c and $2n_c$ (Fig. 2C). We measured

a maximum differential phase shift of 0.07π (12°) when $n_c = 0.1$. The differential amplitude is maximized at a higher $n_c = 0.43$, where it changes by 15% when n_c is increased to $2n_c$ (Fig. 2E). Theoretically, we estimate a maximum of 0.15π (27°) for phase and 20% amplitude modulation with our system parameters.

Conventionally, the intensity-dependent refractive index n_2 or the Kerr coefficient $\chi^{(3)}$ describes the strength of a nonlinear medium in which the nonlinearity is proportional to the photon number (17). The cavity-embedded QD is highly nonlinear and is not well described as a pure Kerr medium. However, for weak excitations, we can still approximate the nonlinear index and susceptibility from the relationship between the acquired signal phase shift ϕ_s and n_2 given by $\phi_s = (2\pi n_2/\lambda_c)(P_{\text{in}}/A_{\text{cav}})(c/2\kappa n)$, where $A_{\text{cav}} \approx (\lambda/n)^2$ is the cavity area, and $c/2\kappa n$ gives the propagation length in GaAs with refractive index $n = 3.5$. From our experimental data at very low values of control power, we infer $n_2 \approx 2.7 \times 10^{-5}$ cm²/W and $\chi^{(3)} = 2.4 \times 10^{-10}$ m²/V². This value is many orders of magnitude larger than most fast optical nonlinearities in solid-state materials.

Spontaneous emission from the QD into modes other than the cavity reduces the per-

formance of quantum gates because of photon losses. In Fig. 2D, we show a 1% photon loss due to incoherent fluorescent emission from the QD, which is driven 0.014 nm away from resonance by the signal laser. Fluorescence loss is expected to scale as $F_{\text{PC}}/(F + F_{\text{PC}}) \approx 0.15\%$, where $F = 160$ is the QD Purcell factor in the PC cavity and $F_{\text{PC}} \approx 0.25$ is the suppression of the QD radiative rate due to the PC lattice (18). The observed 1% is higher than the expected value for losses, but within error, because F_{PC} strongly depends on the dot position and can at most be unity. Radiation from nearby emitters cannot be excluded from this signal and therefore fluorescence losses from the addressed QD may be lower (18).

For applications such as quantum nondemolition (QND) detection and optical control, it is advantageous to spectrally separate the control and signal beams. We detuned the control beam by $\Delta\lambda = -0.027$ nm (1.2g) with respect to the signal beam, which again was aligned to the QD-cavity intersection (Fig. 3A). The number of signal photons per QD lifetime (n_s) was fixed and the control photon number (n_c) was varied. In these measurements, a weakly coupled QD with $g/2\pi \approx \kappa/4\pi = 8$ GHz was used. Saturation power scaled with the modified spontaneous emission

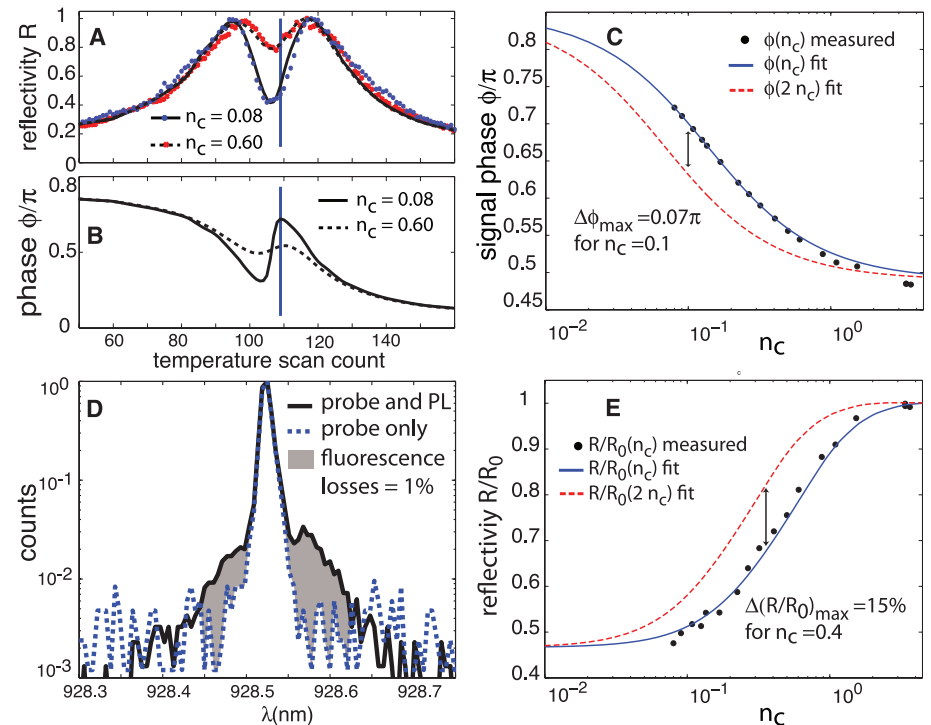


Fig. 2. Nonlinear response of the QD-PC cavity system to single-wavelength excitation near saturation at control photon number $n_c = 0.6$ (A and B). Each temperature scan count corresponds to a particular detuning between the cavity and the QD, as in Fig. 1C. At a detuning of 0.014 nm ($0.3g$) from the dot resonance [vertical line in (B)], the phase changes by 0.24π when n_c increases from 0.08 to 3 (C). The phases derived from experimental scans (points) agree with theory (solid line). The dashed red curve is the fit to experimental results evaluated at control powers of $2n_c$. The signal phase shift due to the doubled signal photon number $\phi(n_c) - \phi(2n_c)$ is maximized at $n_c = 0.1$ (arrow). (D) The main loss mechanism due to fluorescence from the QD corresponds to $\sim 1\%$ photon loss. (E) Reflectivity power dependence. Points correspond to experimental data for reflectivity (R) normalized by the calculated value of R from a cavity with no QD (R_0).

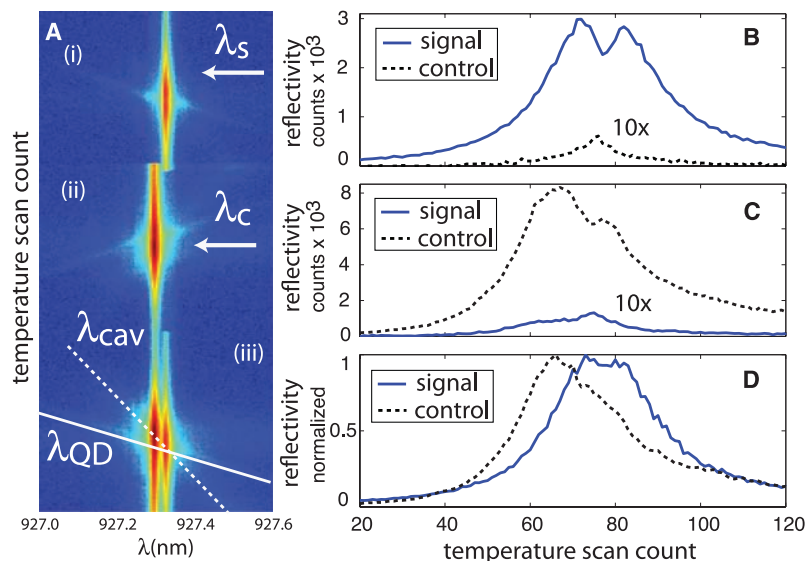


Fig. 3. Interaction between a control and signal beam at different wavelengths. **(A)** The signal beam at λ_s (i) is detuned by 0.027 nm (1.2*g*) from the control beam at λ_c (ii) and positioned to coincide with the cavity-dot crossing-point (iii). For each measurement, a sequence of scans is taken (i to iii). The QD and cavity trajectories are shown in (iii). We track the amplitudes at both wavelengths in each frame (i to iii) to subtract fluorescence backgrounds, which are magnified 10 \times in **(B)** and **(C)** (these are fluorescence backgrounds detected at control and signal wavelengths, respectively). The QD-induced dip is clearly visible in **(B)** when only the signal (solid blue line) is on, and in **(C)** when only the control (dashed line) is on. This feature disappears when both beams are on in **(D)**. In **(D)**, the spectra are normalized to clearly show saturation. The signal and control powers were 100 nW and 200 nW measured before the lens, corresponding to cavity-coupled signal and control photon numbers $n_s \approx 0.2$ and $n_c \approx 0.3$, respectively.

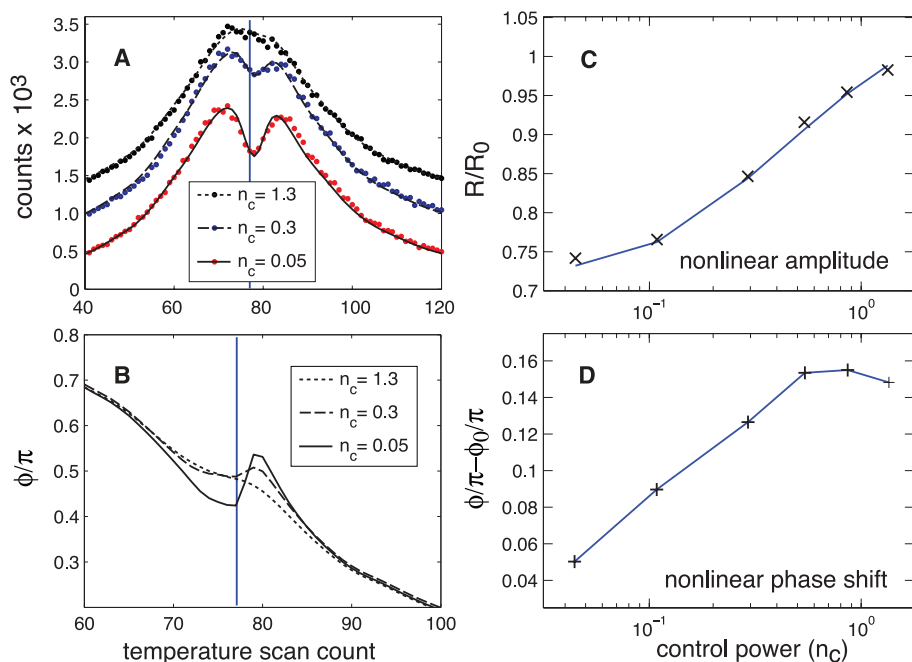


Fig. 4. Nonlinear response of a weakly coupled QD inside the cavity to excitation with control- and signal-beam wavelengths separated by 0.027 nm (1.2*g*). The reflectivity of a signal beam with $n_s = 0.2$ photons per cavity lifetime is shown in **(A)** for three values of the control beam photon number n_c . The QD saturates almost completely when $n_c = 1.3$, which corresponds to a power of 1 μ W measured before the objective lens. The data are fit with a full quantum model, which allows us to extract the signal phase shown in **(B)**. In **(C)**, the amplitude of the reflected signal beam when it is 0.009 nm (0.4*g*) away from the dot resonance [vertical line in **(A)** and **(B)**] is shown as a function of control-beam photon number n_c . In **(D)**, we show the difference between the phase shift of the signal beam when the control beam is on (ϕ) and when it is off (ϕ_0) as a function of n_c at the same time point as in **(C)**.

rate g^2/κ , and so the smaller g value permitted lower control powers and reduced background noise. In Fig. 3, we show the principle of the measurement. First, the signal and control were turned on independently; the QD dip is visible in Fig. 3, B and C. The dip disappeared when the two beams were turned on simultaneously and interacted (Fig. 3D). For better visibility at high control powers, the signal power in Fig. 3 was set to 100 nW before the objective lens, corresponding to $n_s = 0.2$ signal photons in the cavity per cavity lifetime.

In Fig. 4, we show experimental results for phase shifts with control and signal beams at different wavelengths. Here, the signal phase was affected by the saturation of the QD and a frequency shift of the QD due to the ac Stark effect (17), which can be used to realize large phase shifts (19). The signal reflectivity and phase as functions of control-beam photon number are shown in Fig. 4, A and B. We fit both the signal and control data by a full quantum simulation and derived the underlying signal phase shift as a function of the control photon number (20) (see SOM). The reflectivity at the signal wavelength saturated completely when the control photon number reached $n_c = 1.3$, which corresponds to 1 μ W of power measured before the objective lens. The associated phase modulation was 0.13π at the signal detuning of 0.009 nm (0.4*g*) from the dot resonance. The phase behavior in Fig. 4B is asymmetric with respect to the center of the QD-induced dip because the coupling of the control beam changed with the temperature scan.

We fixed the signal wavelength at 0.009 nm ($g/3$) away from the QD resonance and determined the phase and amplitude modulation for a range of values of n_c . The signal phase $\phi(n_c)$ relative to the signal phase with no control $\phi_0 = \phi(n_c = 0)$ is shown in Fig. 4D. The maximum observed phase shift when $n_c = 1$ was 0.16π (28.8°). The largest nonlinear phase change was observed for $n_c = 0.05$, for which $\phi(n_c) - \phi(0) = 0.05\pi$ (9°). These values give a nonlinear index of $n_2 \approx 1.8 \times 10^{-5}$ cm²/W, or $\chi^{(3)} \approx 1.6 \times 10^{-10}$ m²/V², for a detuning of 0.027 nm (1.2*g*) between the signal and control. This value is similar to that of the QD with larger g . Numerical simulations indicate that the relative magnitude of nonlinearities due to these two QDs strongly depends on the laser frequency. The nonlinearities for the two cases are summarized in Table 1.

The current implementation of the QD/cavity system is already promising for low-power and QND photon detectors (8–10). We have shown that the phase and amplitude of the signal strongly depend on the control photon number when the signal and control photons are spectrally separated. Furthermore, the magnitude and bandwidth of the Kerr nonlinearity $\chi^{(3)}$ observed in this experiment are rivaled only by measurements in atomic ensembles (21, 22).

To realize useful quantum logic gates, controlled π phase shifts are necessary (23). This will require repeated interactions. Such cascading

Table 1. Nonlinear parameters and phase modulation derived from experimental data for the strongly (first row) and weakly (second row) coupled QDs. $\Delta\phi$ is a maximum differential phase shift [$\Delta\phi = \phi(n_c) - \phi(0)$], which is achieved at the intracavity photon number n_c in the last column.

| $g/2\pi$ (GHz) | $\lambda_s - \lambda_{\text{QD}}$ (nm) | $\lambda_s - \lambda_c$ (nm) | n_2 (cm ² /W) | $\chi^{(3)}$ (m ² /V ²) | $\Delta\phi$ | n_c |
|----------------|--|------------------------------|----------------------------|--|--------------|-------|
| 16 | 0.014 (0.3g) | 0 | 2.7×10^{-5} | 2.4×10^{-10} | 0.015π | 0.01 |
| 8 | 0.009 (0.4g) | 0.027 | 1.8×10^{-5} | 1.6×10^{-10} | 0.05π | 0.05 |

requires coupling efficiencies that are higher than the observed 2 to 5%. This technical challenge can be overcome. We have already demonstrated architecture for a QD cavity-waveguide-coupled quantum network (24) with coupling efficiency above 50% between two nodes, and cavity-waveguide couplers (25) with coupling efficiency reaching 90%. The observed fluorescence losses are already sufficiently low to allow scalable computation (26), and can be further improved with increases in cavity Q. The ability to tailor photon-QD interactions by PC fabrication makes this a highly versatile platform for a variety of quantum optics experiments and has great potential for compact scalable quantum devices.

References and Notes

- E. Knill, R. Laflamme, G. J. Milburn, *Nature* **409**, 46 (2001).
- Q. Turchette, C. Hood, W. Lange, H. Mabuchi, H. J. Kimble, *Phys. Rev. Lett.* **75**, 4710 (1995).

- T. Wilk, S. C. Webster, A. Kuhn, G. Rempe, *Science* **317**, 488 (2007).
- J. Majer *et al.*, *Nature* **449**, 443 (2007).
- C. Santori *et al.*, *Phys. Rev. Lett.* **97**, 247401 (2006).
- M. V. Gurudev Dutt *et al.*, *Science* **316**, 1312 (2007).
- D. P. DiVincenzo, *Fortschr. Phys.* **48**, 771 (2000).
- N. Imoto, H. Haus, Y. Yamamoto, *Phys. Rev. A* **32**, 2287 (1985).
- J. P. Poizat, P. Grangier, *Phys. Rev. Lett.* **70**, 271 (1993).
- G. Nogues *et al.*, *Nature* **400**, 239 (1999).
- Y. Akahane, T. Asano, B.-S. Song, S. Noda, *Nature* **425**, 944 (2003).
- D. Englund *et al.*, *Nature* **450**, 857 (2007).
- H. Altug, J. Vučković, *Opt. Lett.* **30**, 982 (2005).
- E. Waks, J. Vučković, *Phys. Rev. Lett.* **96**, 153601 (2006).
- I. L. Chuang, Y. Yamamoto, *Phys. Rev. A* **52**, 3489 (1995).
- K. N. W. J. Munro, T. Spiller, *N. J. Phys.* **7**, 137 (2005).
- R. Boyd, *Nonlinear Optics* (Academic Press, New York, ed. 2, 2003).
- D. Englund *et al.*, *Phys. Rev. Lett.* **95**, 013904 (2005).
- E. Waks, J. Vučković, *Phys. Rev. A* **73**, 041803 (2006).
- S. M. Tan, www.qo.phy.auckland.ac.nz/qotoolbox.html.

- S. Harris, J. Field, A. Imamoglu, *Phys. Rev. Lett.* **64**, 1107 (1990).
- K.-J. Boller, A. Imamoglu, S. E. Harris, *Phys. Rev. Lett.* **66**, 2593 (1991).
- M. A. Nielsen, I. L. Chuang, *Quantum Computation and Quantum Information* (Cambridge Univ. Press, Cambridge, UK, 2000).
- D. Englund, A. Faraon, B. Zhang, Y. Yamamoto, J. Vučković, *Opt. Express* **15**, 5550 (2007).
- A. Faraon, E. Waks, D. Englund, I. Fushman, J. Vučković, *Appl. Phys. Lett.* **90**, 073102 (2007).
- E. Knill, *Nature* **434**, 39 (2005).
- Financial support was provided by the Multidisciplinary University Research Incentive Center for photonic quantum information systems (Army Research Office/Intelligence Advanced Research Projects Agency Program DAAD19-03-1-0199), Office of Naval Research Young Investigator Award, and NSF grant CCF-0507295. D.E. and I.F. were also supported by a National Defense Science and Engineering Graduate fellowship. Part of the work was performed at the Stanford Nanofabrication Facility of the National Nanotechnology Infrastructure Network supported by the NSF under grant ECS-9731293.

Supporting Online Material

www.sciencemag.org/cgi/content/full/320/5877/1769/DC1
SOM Text

Figs. S1 and S2

References and Notes

26 December 2007; accepted 1 April 2008
10.1126/science.1154643

Conditional Dynamics of Interacting Quantum Dots

Lucio Robledo,¹ Jeroen Elzerman,¹ Gregor Jundt,¹ Mete Atatüre,² Alexander Högele,¹ Stefan Fält,¹ Atac Imamoglu^{1*}

Conditional quantum dynamics, where the quantum state of one system controls the outcome of measurements on another quantum system, is at the heart of quantum information processing. We demonstrate conditional dynamics for two coupled quantum dots, whereby the probability that one quantum dot makes a transition to an optically excited state is controlled by the presence or absence of an optical excitation in the neighboring dot. Interaction between the dots is mediated by the tunnel coupling between optically excited states and can be optically gated by applying a laser field of the right frequency. Our results represent substantial progress toward realization of an optically effected controlled-phase gate between two solid-state qubits.

Self-assembled semiconductor quantum dots (QDs) (1) can be manipulated and probed optically, enabling ultrafast coherent control (2) and rendering them model systems for solid-state quantum optics (3). Particularly promising are quantum dots deterministically charged with a single electron, because the electron spin state is robust against relaxation and decoherence (4). In such systems, single-electron spin states can be optically prepared (5) and read out (6, 7), allowing demonstrations of optically

detected electron spin resonance (8) and coherent spin dynamics (9). These results established QD spins as promising candidates for solid-state qubits and motivated our research aimed at demonstrating conditional interactions, which is required for implementing two-qubit quantum gates.

In electrically defined QDs, the exchange interaction (10) has been used to demonstrate such controlled conditional coupling between electron spins (11). However, this mechanism requires fast electrical control over the exchange splitting, which is not feasible in self-assembled QDs (12–14). An alternative mechanism that has been proposed for coherent coupling of self-assembled QDs (15) is based on dipole-dipole interaction (16), which can be switched on in sub-picosecond time scales by optically exciting

both QDs (17). However, for standard vertically coupled QDs, the bare dipole-dipole interaction is typically too weak (smaller than the linewidth of a QD transition) to allow for the accumulation of large conditional phase shifts.

We present an experimental realization of a strong optically gated interaction between a neutral and a single-electron-charged QD. The interaction mechanism, which relies on the tunnel coupling between the dots (12–14), is tunable and can be much larger than the dipole-dipole interaction. The experiments were performed in a GaAs device (grown by molecular beam epitaxy), containing two layers of self-assembled InGaAs QDs with a nominal separation of 15 nm. QDs in the top layer tend to grow directly on top of QDs in the bottom layer because of the strain field produced by the latter (14), resulting in stacks of vertically coupled QDs (CQDs). These QD stacks are embedded in a field-effect structure consisting of an n⁺-doped GaAs layer acting as an electron reservoir (with a 25-nm tunnel barrier to the bottom QD layer) and a 4-nm-thick semi-transparent Ti top gate (Fig. 1A). By varying the gate voltage, we can deterministically charge the two dots and tune their relative energy. In order to reach a regime where the electronic energy levels of a stack can be brought into resonance, the size of the bottom QDs has been reduced during growth, leading to an increase of their recombination energy. In the following, we refer to the QDs of a stack as the blue QD (bottom) and the red QD (top). The relatively thick tunnel barrier between the dots [compared with the CQDs used in (12, 13)] assures that

¹Institute of Quantum Electronics, Eidgenössische Technische Hochschule (ETH)–Zürich, CH-8093 Zürich, Switzerland.
²Cavendish Laboratory, University of Cambridge, J. J. Thomson Avenue, Cambridge CB3 0HE, UK.

*To whom correspondence should be addressed. E-mail: imamoglu@phys.ethz.ch